Manipulation of Electrode Composition for Effective Water Management in Fuel Cells Fed with an Electrically Rechargeable Liquid Fuel

Xingyi Shi[1], Xiaoyu Huo[1], Oladapo Christopher Esan[1], Yichen Dai[1], Liang An*[, 1], T.S. Zhao*[, 2]

[1] Department of Mechanical Engineering, The Hong Kong Polytechnic University, Hung Hom, Kowloon, Hong Kong SAR, China

[2] Department of Mechanical and Aerospace Engineering, The Hong Kong University of Science and Technology, Clear Water Bay, Kowloon, Hong Kong SAR, China

* Corresponding authors.

Email: liang.an@polyu.edu.hk (L. An)

Email: metzhao@ust.hk (T.S. Zhao)

Abstract

Liquid fuel cell, with its high energy density and ease of fuel handling, has attracted great attention world-wide. However, its real application is still being greatly hindered by its limited power density. Hence, the recently proposed and demonstrated fuel cell, using an electrically rechargeable liquid fuel (e-fuel), is believed to be a candidate with great potential due to its significant performance advancement. Unlike the conventional alcoholic liquid fuels, the e-fuel possesses excellent reactivity, even on carbon-based materials, which therefore allows the e-fuel cell to achieve superior performance without any noble metal catalysts. However, it is found that, during the cell operation, the water generated at the cathode following the oxygen reduction reaction could lead

to water flooding problem and further limit the cell performance. To address this issue, in this work, by manipulating the cathode composition, a blended binder cathode using both Nafion and polytetrafluoroethylene (PTFE) as binding agents is fabricated and demonstrated its superiority in the fuel cell to achieve an enhanced water management and cell performance. Furthermore, using the developed cathode, a fuel cell stack is designed and fabricated to power a 3D-printed toy car, presenting this system as a promising device feasible for future study and real applications.

Key words: E-fuel; Fuel cell; Stack; Water flooding; Water management

1. Introduction

Due to the rapid change of climate and imminent energy crisis, the development of renewable energy to replace conventional fossil fuels for power generation has become an imperative option across the globe in the last decades.[1-3] Among the diverse types of renewable power generation systems, the proton exchange membrane fuel cell (PEMFC) using hydrogen and oxygen for electricity production has received an increasing attention.[4, 5] The PEMFC possesses a lot of advantages including high efficiencies, zero emission, and fast refueling.[6, 7] However, up till now, the production, storage, and transportation of hydrogen still lack effective solutions and hence greatly restrict the commercialization progress of PEMFCs.[8] Alternatively, direct liquid fuel cells (DLFCs) using liquid alcohols have made notable progress and are considered to be a promising power generation candidate.[9-11] However, while the DLFCs cracked the fuel transportation difficulties faced by PEMFCs, by using liquid fuels, their limited power densities are still far from practical application requirements.[11]

Recently, a novel fuel cell using the electrically rechargeable fuel (e-fuel) for power generation has been demonstrated.[12, 13] The e-fuel can be made of a wide range of electroactive materials. In our previous studies, we developed a liquid e-fuel cell employing vanadium-based e-fuel and oxygen as reactants,[14-18] and demonstrated its power generation capability under different operating conditions. While the cell is proved to exhibit a substantially improved performance which exceeds other conventional direct alcohol fuel cells, it is found that the water generated at the cathode during the cell operation due to the oxygen reduction reaction could lead to water

flooding problem.[19] Such a phenomenon would block the reactive sites at the cathode and further impede the mass transport of reactive species, which thereby could lead to unstable and limited cell performance, especially at low oxidant flow rates.[19]

Hence, in this work, to resolve the water flooding problem in the fuel cell, polytetrafluoroethylene (PTFE) as one of the widely used hydrophobic binding agents,[20, 21] has been blended with Nafion and used as the binder for cathode fabrication. It is believed that the PTFE not only helps with the excessive water removal to avoid water flooding problem during the cell operation, but also reduces the cathode production cost due to its cheaper price in comparison to Nafion.[21] Using this blended binder cathode, a fuel cell with an improved cell stability and a higher peak power density in comparison to the cell using pure Nafion for the cathode is demonstrated. Furthermore, an e-fuel cell stack, using the blended binder cathode, has also been designed and fabricated, of which an excellent performance consistency between its two individual cells is found and is capable of powering a 3D-printed toy car. The significant cell performance and demonstration achieved in this work thus present the fuel cell as a promising device feasible for future real-world applications.

2. Working principle

As shown in **Fig. 1**, a catalyst-free graphite-felt anode, a Pt/C coated oxygen cathode, and a proton exchange membrane constitute the membrane electrode assembly (MEA) inside the fuel cell. While the vanadium ion oxidation reaction occurs at anode, oxygen reduction reaction takes place at cathode and water is then produced. The overall reaction is thus as shown below:

$$V^{2+} + \frac{1}{4}O_2 + H^+ \rightarrow V^{3+} + \frac{1}{2}H_2O \qquad \Delta E = 1.49V$$

3. Experimental

3.1. Preparation of the membrane electrode assembly

The home-made MEA used in this work consisted of an anode, a cathode and a Nafion 211 membrane in the middle. The graphite felt (AvCarb G100, Fuel Cell Store) was thermally treated in the air for 5 hours at 500˚C before its usage as the anode to enhance its hydrophilicity and activity. Meanwhile, the Pt/C coated carbon paper cathodes were prepared following the previously reported method.[13] The catalyst ink was first prepared by mixing 60 wt. % Pt/C (Johnson Matthey Co., USA) as catalyst, 5 wt. % Nafion (Fuel Cell Store, USA) and 60 wt. % PTFE (Fuel Cell Store, USA) of different weight ratios as binder, and ethanol as solvent. Afterwards, the ink was sprayed onto the carbon paper to form the catalyst layer with a metallic loading of 2.0 mg cm^{-2}. In this work, by altering the binder compositions during ink preparation, three types of cathodes using 100 wt.% Nafion, 50 wt.% Nafion and 50 wt.% PTFE, and 100 wt.% PTFE were prepared and are denoted as $Nafion_{1.0}$, $Nafion_{0.5}PTFE_{0.5}$, and $PTFE_{1.0}$, respectively. The Nafion 211 membrane was pretreated following the reported standard procedure to ensure high proton conductivity and reduce the membrane area resistance, which in turn lowers the ohmic polarization loss of the cell for better performance.[13]

3.2. Experimental apparatus

The surface morphologies and hydrophobicity of each fabricated cathode were characterized by the field emission scanning electron microscope (SEM) (Tescan VEGA3, Czechoslovakia) and the contact angle test instrument (Theta Flex, Biolin,

Sweden), respectively. The transparent fuel cell was designed and fabricated using a transparent acrylic plate to visualize the water flooding phenomenon at the cathode. During the test, the e-fuel is delivered to the anode by a peristaltic pump at a flow rate of 60 mL min^{-1} from a tank of 120 mL e-fuel, while pure oxygen was fed to the cathode at a flow rate of 10 sccm. The polarization curve tests were conducted using another home-made active[13-15] and passive fuel cells[16] as reported before, both of which have an active area of 2.0*2.0 cm^2. For the active fuel cell, the e-fuel and the oxygen were fed into the cell at 60 mL min^{-1} and 10 sccm, respectively. While for the passive fuel cell, a current collector with an open ratio of 70 % was adopted.[16] Both cells used 20 mL e-fuel during the tests. The stack performance was investigated with a home-made fuel cell stack, which consists of two individual passive fuel cells each with 20 mL e-fuel tank. The active area of each individual cell in the stack was 2.0*4.0 cm^2. For all the tests, the e-fuel was prepared by first dissolving $VOSO_4$ in H_2SO_4 and then charging it using a typical flow cell. The polarization and constant-current discharging tests were carried out using an Arbin BT2000 (Arbin Instrument Inc.). All the experiments were performed under room temperature.

4. Results and Discussion

4.1 Characterization of the electrodes

Excellent water management has been well recognized as a critical requirement to provide the fuel cell with superior performance.[22, 23] On the one hand, good wettability of the electrode plays significant influence towards securing a suitable humidity to ensure adequate membrane hydration level and thereby allowing the ease of ion

conduction and a lower ohmic loss.[22] However, it is also required for the electrode to be capable of removing excess liquid water so as to prevent water flooding.[24] Hence, in this work, to achieve a balance between adequate membrane hydration level and cathode water removal ability, the hydrophobic PTFE has been blended with the hydrophilic Nafion during the catalyst ink preparation for the cathode fabrication.[25] Then, to investigate the effects of the binder compositions on the hydrophilicity of the cathode catalyst layer, the water contact angles of the prepared cathodes have also been tested as shown in **Figs. 2 (a-c)**. It is observed that, a contact angle of 140.00˚, 152.99˚, and 158.42˚ is presented for the $Nafion_{1.0}$, $Nafion_{0.5}PTFE_{0.5}$, and $PTFE_{1.0}$ cathodes, respectively. Such result thereby suggests that the use of more PTFE during electrode fabrication can result in better hydrophobicity as expected, which thereafter can enhance the water removal ability of the cathode.[24] Furthermore, to examine the effects of the binder composition on the surface morphologies of the cathodes, the SEM images of the three cathodes have also been captured. As presented in **Fig. S1 (a-c)**, no obvious morphology change is found, which thereby demonstrates that the addition of PTFE to Nafion does not make any significant influence on the cathode catalyst layer structure.

4.2 General Performance

In this work, to address the water flooding issue, the hydrophobic PTFE ionomer has been blended with the conventional Nafion resin and used as the binding agents to fabricate a blended binder cathode. The fabricated $Nafion_{0.5}PTFE_{0.5}$ cathode using a blended binder of 50% wt. Nafion and 50% wt. PTFE is then examined and the results are as shown in **Figs. 3 (a) and (c)**. It can be seen that, with the active and passive cell

design, a peak power density of 552.68 and 120.90 mW cm^{-2} has been demonstrated, respectively. Such a superior performance not only exceeds that of the pure Nafion/PTFE cathodes as presented below, but also substantially surpasses those of the conventional alcohol fuel cells (**Figs. 3 (b) and (d)**). Thus, with the advantages of achieving a balance between an adequate membrane hydration level and a satisfactory cathode water removal ability as demonstrated in the following sections, this presented blended binder cathode is believed to be a promising candidate for future use. Furthermore, this fuel cell system should be considered as a powerful competitor with promising potential for practical applications.

4.3 Visualizations of the cathode water flooding

As discussed previously, the water flooding problem at the cathode could severely deteriorate the cell performance.[26] Hence, to evaluate the impact of the prepared cathodes on the cell performance and demonstrate their abilities for water removal, a fuel cell with a transparent cathode flow field has been designed and fabricated (**Fig. 4 (a)**) to enable the visualizations of the water flooding phenomenon. Three cathodes of different binder compositions have been assembled into the cell for the analysis and the results are as shown in **Figs. 4 (b-c)**. It can be seen that, when $Nafion_{1.0}$ is tested, the cell can only be operated for ~50 mins before the cell voltage drops to 0.5 V. Such a limited cell performance is mainly caused by the poor water removal ability of the cathode as evidenced in **Fig. 4 (c)**, where obvious water flooding phenomenon can be seen especially at points A_4 and A_5. It is attributed to the presence of excessive liquid water which not only covers the active reaction surface, but also impedes the transport

of oxygen molecules, resulting in insufficient oxidant feeding and thereby leading to the sudden voltage drop.[27] In order to further justify this conclusion, immediately after the cell voltage drops to 0.5V the oxygen flow rate has been increased from 10 to 500 sccm and as shown **Fig. S2**, a sudden voltage jump can be seen right after the change of the oxygen flow rate and the cell is found to be capable of operating stably thereafter. Such a phenomenon therefore again proves that the limited cell performance using $Nafion_{1.0}$ arises from the poor cathode water removal ability while the high oxygen flow rate can help with the water removal due to the enhanced gas sweeping effect on the liquid water, which thereby alleviate the water flooding issue.[28] In contrast, for the fuel cell using $Nafion_{0.5}PTFE_{0.5}$ and $PTFE_{1.0}$ cathodes, the cell is found to be capable of operating stably for three hours under the same operating condition. Furthermore, as shown in the photos (**Fig. 4 (c)**), the cathode flow channels are also found to be relatively dry during the whole test, which thereby proves the improved water removal ability of the cathode with the addition of PTFE during the electrode fabrication. In summary, water flooding is found to be of critical issue which could influence and limit the cell performance, however, the $Nafion_{0.5}PTFE_{0.5}$ and $PTFE_{1.0}$ cathodes have been proven to ease water removal during the cell operation.

4.4 Effect of the cathode binder composition

The wettability of the cathode not only closely relates to its water removal ability but also plays a pivotal role in influencing the membrane hydration level, which further determines the cell performance.[26] Hence, to further evaluate the effects of the binder compositions, the polarization tests have been conducted for cells assembled with three

different cathodes, as shown in **Fig. 5**. It can be seen that, with both the active (**Fig. 5 (a-b)**) and passive (**Fig. 5 (c-d)**) fuel cell designs, $Nafion_{0.5}PTFE_{0.5}$ cathode is demonstrated to achieve the best cell performance. Such a result is due to that the $Nafion_{0.5}PTFE_{0.5}$ cathode can achieve a more balanced membrane hydration level and cathode water removal ability.[29] In comparison to $Nafion_{0.5}PTFE_{0.5}$, the $Nafion_{1.0}$ cathode due to its better wettability can ensure the membrane with higher ionic conductivity and thereby a lower ohmic loss.[19, 22] However, it can also result in the difficulty of removing excess water generated during cell operation, which thereafter hampers the oxidant delivery and further deteriorates the cell performance. In contrast, the $PTFE_{1.0}$ cathode, though grants better oxidant delivery, also results in larger ohmic loss and thereby limits the cell performance as it adversely influences the membrane hydration level.[30] Therefore, overall, the $Nafion_{0.5}PTFE_{0.5}$ cathode with its best performance among all the cathodes tested and lower price than the $Nafion_{1.0}$ cathode, is believed to possess great potential for future applications. It is also worth mentioning that, when tested in the passive fuel cell, the $PTFE_{1.0}$ cathode demonstrate a better and preferable performance in comparison to the $Nafion_{1.0}$ cathode, which thereby proves the significant effects of water flooding on the passive fuel cell performance.

4.5 General stack performance

As proved in the previous sections, using the $Nafion_{0.5}PTFE_{0.5}$ cathode, this presented fuel cell is found to achieve a performance exceeding that of conventional direct liquid fuel cells. Hence, to demonstrate the potential of this fuel cell for real application, in this work, a liquid fuel cell stack consisting of two cells has been designed and

fabricated as shown in **Fig. 6 (a-b)**. To begin with, in order to confirm the performance consistency of individual cell, independent tests have been conducted on both cells under the same operating condition and the results are as presented in **Fig. 6 (c)**. It is observed that the two individual cells show an excellent performance consistency over the whole tested current range, which thereby proves the good reproducibility of the fabricated cell and justifies its potential for mass production and wide application in future.[9] On top of this, the performance of the whole stack has also been investigated as shown in **Fig. 6 (d)**. It is found that the whole stack is able to generate an open circuit voltage of 2.37 V, a peak power of 1771.8 mW, and a maximum current of 1441 mA. Such a superior performance, that outperforms the majority of conventional liquid alcohol cell stacks at the same size in the open literatures,[31-33] therefore presents this system to be of great potential in realizing practical applications in the future.

4.6 Demonstration of the passive stack to power a toy car

To further exhibit the application potential of this system, as a prototype demonstration, a home-made toy car powered by the prepared liquid fuel cell stack is designed and then fabricated using the 3D printing technology, as shown in **Fig. 7 (a-b)**. Before starting, the constant-current discharging test has been first performed for the liquid fuel cell stack and the results are shown in **Fig. 7 (c)**. During the operation at 20 mA, the stack exhibits a stable operation for ~5 hours indicating the capability of this cell for continuous power generation. Afterwards, when assembled into the toy car, it can be seen in **Video S1** that the stack is capable of generating enough power to drive the toy car stably. Such a result therefore again suggests that this fuel cell stack is of great

potential to achieve real application such as powering the future fuel cell electric vehicles. However, it is worth mentioning that, one major limitation of this system is its relatively low energy efficiency of 12.55 %, which may be attributed to the reactive species crossover issue and the undesired side reaction at the anode side as reported before,[16] both of which can result in the loss of fuel capacity. Therefore, it is suggested that future studies are still required to address these problems before realizing the widespread commercialization of this system.

5. Conclusion

In this work, by manipulating the cathode composition, a blended binder PTFE/Nafion cathode is fabricated and examined in an e-fuel cell. It is found that, introducing PTFE during cathode fabrication not only allows a more balanced membrane hydration level and cathode water removal ability, but also reduces the cathode production cost, which thereby grants the cell higher peak power density, better stability, and lower capital cost. Furthermore, to demonstrate the application potential of this system, a liquid e-fuel cell stack consisting of two individual cells has also been designed and fabricated. This stack is found to exhibit an excellent performance consistency for its two individual cells and is capable of powering a toy car, which therefore presents this system as a promising device feasible for future study and real applications. However, it is also found that the energy efficiency of this stack is still limited, which thereby requires future investigations.

Conflicts of interest

There are no conflicts to declare.

Supporting Information

Surface morphologies of $Nafion_{1.0}$, $Nafion_{0.5}PTFE_{0.5}$, and $PTFE_{1.0}$ cathodes; constant-current discharging behavior of the transparent fuel cell assembled with $Nafion_{1.0}$ cathode; table with detailed comparison of power densities among various liquid fuel cells; and video of a 3D-printed toy car powered by the passive fuel cell stack.

Acknowledgement

The work described in this paper was fully supported by a grant from the Research Grant Council of the Hong Kong Special Administrative Region, China (Project No. T23-601/17-R).

References

1. J. Liu, Q. Ma, Z. Huang, G. Liu and H. Zhang, Recent Progress in Graphene-based Noble-metal Nanocomposites for Electrocatalytic Applications, *Advanced Materials*, 2019, **31**, 1800696.
2. D. Larcher and J.-M. Tarascon, Towards Greener and More Sustainable Batteries for Electrical Energy Storage, *Nature Chemistry*, 2015, **7**, 19-29.
3. W. Liu, W. Mu, M. Liu, X. Zhang, H. Cai and Y. Deng, Solar-induced Direct Biomass-to-electricity Hybrid Fuel Cell Using Polyoxometalates as Photocatalyst and Charge Carrier, *Nature Communications*, 2014, **5**, 1-8.
4. K. Jiao, J. Xuan, Q. Du, Z. Bao, B. Xie, B. Wang, Y. Zhao, L. Fan, H. Wang and Z. Hou, Designing the Next Generation of Proton-exchange Membrane Fuel Cells, *Nature*, 2021, **595**, 361-369.
5. A. Holewinski, J.-C. Idrobo and S. Linic, High-performance Ag–Co Alloy Catalysts for Electrochemical Oxygen Reduction, *Nature Chemistry*, 2014, **6**, 828-834.
6. T. Tamaki, H. Kuroki, S. Ogura, T. Fuchigami, Y. Kitamoto and T. Yamaguchi, Connected Nanoparticle Catalysts Possessing a Porous, Hollow Capsule Structure as Carbon-free Electrocatalysts for Oxygen Reduction in Polymer Electrolyte Fuel Cells, *Energy & Environmental Science*, 2015, **8**, 3545-3549.
7. X. X. Du, Y. He, X. X. Wang and J. N. Wang, Fine-grained and Fully Ordered Intermetallic PtFe Catalysts with Largely Enhanced Catalytic Activity and Durability, *Energy & Environmental Science*, 2016, **9**, 2623-2632.
8. Ö. Atlam and G. Dündar, A Practical Equivalent Electrical Circuit Model for Proton Exchange Membrane Fuel Cell (PEMFC) Systems, *International Journal of Hydrogen Energy*, 2021, **46**, 13230-13239.
9. Z. Pan, H. Zhuang, Y. Bi and L. An, A Direct Ethylene Glycol Fuel Cell Stack as Air-independent Power Sources for Underwater and Outer Space Applications, *Journal of Power Sources*, 2019, **437**, 226944.
10. B. Ong, S. Kamarudin and S. Basri, Direct Liquid Fuel Cells: A Review, *International Journal of Hydrogen Energy*, 2017, **42**, 10142-10157.
11. S. Giddey, S. Badwal, A. Kulkarni and C. Munnings, A Comprehensive Review of Direct Carbon Fuel Cell Technology, *Progress in Energy and Combustion Science*, 2012, **38**, 360-399.
12. H. Jiang, L. Wei, X. Fan, J. Xu, W. Shyy and T. Zhao, A Novel Energy Storage System Incorporating Electrically Rechargeable Liquid Fuels as the Storage Medium, *Science Bulletin*, 2019, **64**, 270-280.
13. X. Shi, X. Huo, Y. Ma, Z. Pan and L. An, Energizing Fuel Cells with an Electrically Rechargeable Liquid Fuel, *Cell Reports Physical Science*, 2020, **1**, 100102.
14. X. Shi, X. Huo, O. C. Esan, Y. Ma, L. An and T. Zhao, A Liquid E-fuel Cell Operating at− 20° C, *Journal of Power Sources*, 2021, **506**, 230198.
15. X. Shi, X. Huo, O. C. Esan, L. An and T. Zhao, Performance Characteristics of a Liquid E-fuel Cell, *Applied Energy*, 2021, **297**, 117145.

16. X. Shi, Y. Dai, O. C. Esan, X. Huo, L. An and T. Zhao, A Passive Fuel Cell Fed with an Electrically Rechargeable Liquid Fuel, *ACS Applied Materials & Interfaces*, 2021, **13**, 48795-48800.
17. O. C. Esan, X. Shi, X. Su, Y. Dai, L. An and T. Zhao, A Computational Model of a Liquid E-fuel Cell, *Journal of Power Sources*, 2021, **501**, 230023.
18. O. C. Esan, X. Shi, Y. Dai, L. An and T. Zhao, Operation of Liquid E-fuel Cells Using Air As Oxidant, *Applied Energy*, 2022, **311**, 118677.
19. P. C. Okonkwo and C. Otor, A Review of Gas Diffusion Layer Properties and Water Management in Proton Exchange Membrane Fuel Cell System, *International Journal of Energy Research*, 2021, **45**, 3780-3800.
20. X. Zhang and P. Shi, Nafion Effect on Dual-bonded Structure Cathode of PEMFC, *Electrochemistry Communications*, 2006, **8**, 1615-1620.
21. Z. Pan, Y. Bi and L. An, A Cost-effective and Chemically Stable Electrode Binder for Alkaline-acid Direct Ethylene Glycol Fuel Cells, *Applied Energy*, 2020, **258**, 114060.
22. P. K. Das, X. Li and Z.-S. Liu, Analysis of Liquid Water Transport in Cathode Catalyst Layer of PEM Fuel Cells, *International Journal of Hydrogen Energy*, 2010, **35**, 2403-2416.
23. J. W. Bae, Y.-H. Cho, Y.-E. Sung, K. Shin and J. Y. Jho, Performance Enhancement of Polymer Electrolyte Membrane Fuel Cell by Employing Line-patterned Nafion Membrane, *Journal of Industrial and Engineering Chemistry*, 2012, **18**, 876-879.
24. B. Chi, S. Hou, G. Liu, Y. Deng, J. Zeng, H. Song, S. Liao and J. Ren, Tuning Hydrophobic-hydrophilic Balance of Cathode Catalyst Layer to Improve Cell Performance of Proton Exchange Membrane Fuel Cell (PEMFC) by Mixing Polytetrafluoroethylene (PTFE), *Electrochimica Acta*, 2018, **277**, 110-115.
25. K. Lee, S. Ferekh, A. Jo, S. Lee and H. Ju, Effects of Hybrid Catalyst Layer Design on Methanol and Water Transport in a Direct Methanol Fuel Cell, *Electrochimica Acta*, 2015, **177**, 209-216.
26. H. Li, Y. Tang, Z. Wang, Z. Shi, S. Wu, D. Song, J. Zhang, K. Fatih, J. Zhang and H. Wang, A Review of Water Flooding Issues in the Proton Exchange Membrane Fuel Cell, *Journal of Power Sources*, 2008, **178**, 103-117.
27. T. Van Nguyen and G. Lin, Effect of Morphological and Wetting Characteristics of the Gas Diffusion Layers on Electrode Flooding Level in a PEM Fuel Cell, *ECS Proceedings Volumes*, 2004, **2004**, 412.
28. D. Natarajan and T. Van Nguyen, Current Distribution in PEM Fuel Cells. Part 1: Oxygen and Fuel Flow Rate Effects, *AIChE Journal*, 2005, **51**, 2587-2598.
29. G. S. Avcioglu, B. Ficicilar and I. Eroglu, Effect of PTFE Nanoparticles in Catalyst Layer with High Pt Loading on PEM Fuel Cell Performance, *International Journal of Hydrogen Energy*, 2016, **41**, 10010-10020.
30. W. Dai, H. Wang, X.-Z. Yuan, J. Martin, J. Shen, M. Pan and Z. Luo, Measurement of Water Transport Rates across the Gas Diffusion Layer in a Proton Exchange Membrane Fuel Cell, and the Influence of Polytetrafluoroethylene Content and Micro-porous Layer, *Journal of Power*

Sources, 2009, **188**, 122-126.
31. Y. S. Li and T. S. Zhao, A Passive Anion-exchange Membrane Direct Ethanol Fuel Cell Stack and its Applications, *International journal of hydrogen energy*, 2016, **41**, 20336-20342.
32. X. Li and A. Faghri, Development of a Direct Methanol Fuel Cell Stack Fed with Pure Methanol, *International journal of hydrogen energy*, 2012, **37**, 14549-14556.
33. D. Chu and R. Jiang, Effect of Operating Conditions on Energy Efficiency for a Small Passive Direct Methanol Fuel Cell, *Electrochimica Acta*, 2006, **51**, 5829-5835.

Figure captions:

Fig. 1 Working principle of a liquid fuel cell.

Fig. 2 Contact angles of (a) $Nafion_{1.0}$, (b) $Nafion_{0.5}PTFE_{0.5}$, and (c) $PTFE_{1.0}$ cathodes, respectively.

Fig. 3 General performance and peak power density comparison of (a-b) active and (c-d) passive fuel cells with the data available in the open literature.

Fig. 4 (a) Design of a fuel cell with a transparent cathode endplate. (b) Constant-current discharging behaviors and (c) visualization of flow channel with three cathodes.

Fig. 5 Experimental set-up and polarization & power density curves of (a-b) the active and (c-d) the passive fuel cell assembled with three cathodes.

Fig. 6 (a) Design and (b) fabrication of a fuel cell stack. (c) The consistency of two individual cells. (d) General performance of this passive fuel cell stack.

Fig. 7 (a) Design and (b) fabrication of a fuel cell powered toy car. (c) Constant-current discharging behaviors of the fuel cell stack.

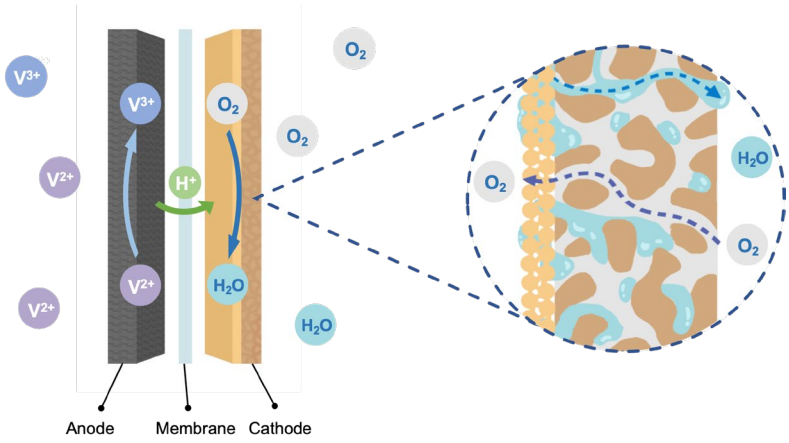

Fig. 1 Working principle of a liquid fuel cell.

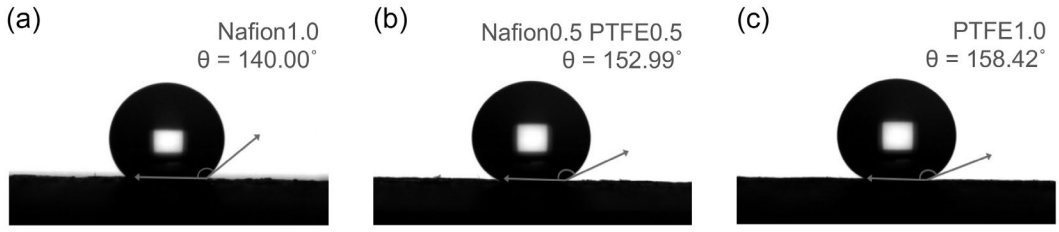

Fig. 2 Contact angles of (a) $Nafion_{1.0}$, (b) $Nafion_{0.5}PTFE_{0.5}$, and (c) $PTFE_{1.0}$ cathodes, respectively.

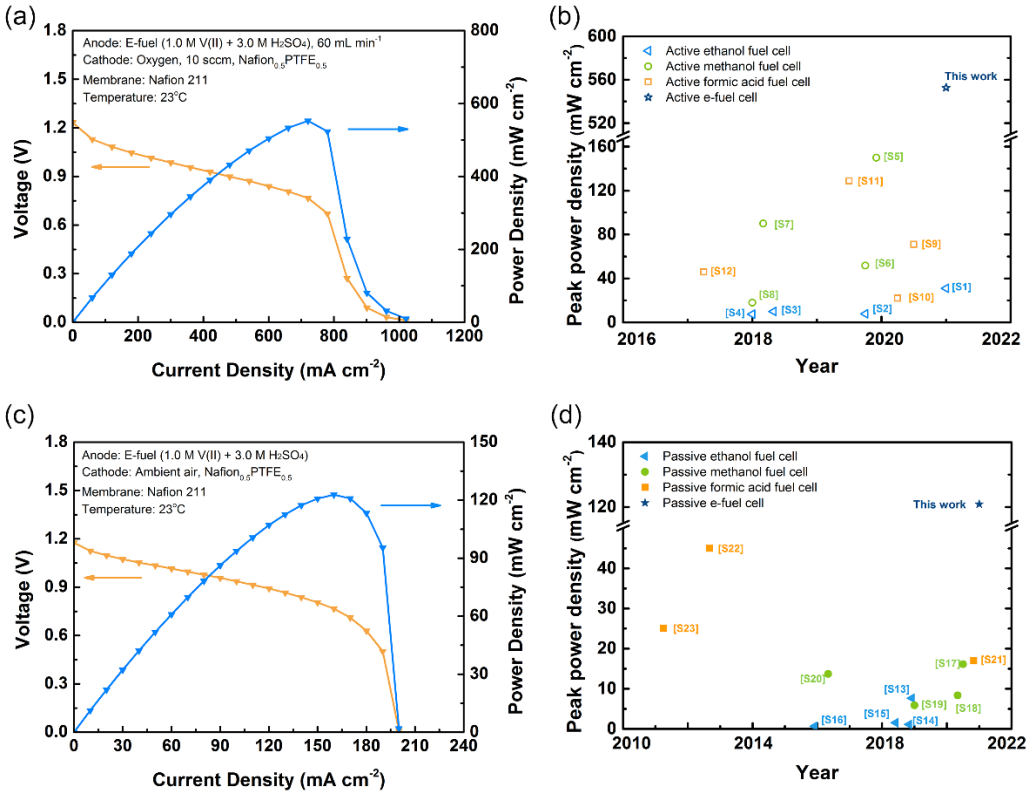

Fig. 3 General performance and peak power density comparison of (a-b) active and (c-d) passive fuel cells with the data available in the open literature.

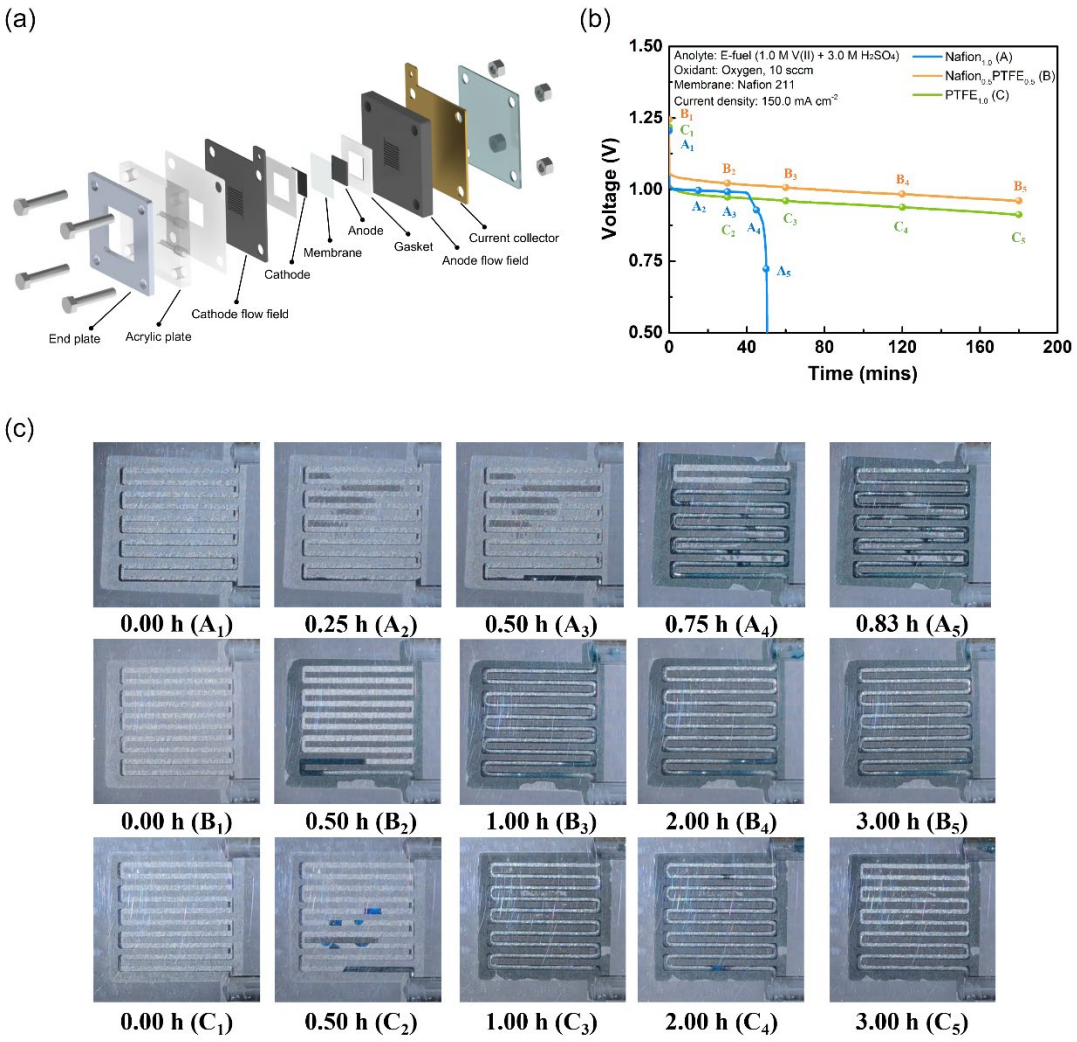

Fig. 4 (a) Design of a fuel cell with a transparent cathode endplate. (b) Constant-current discharging behaviors and (c) visualization of flow channel with three cathodes.

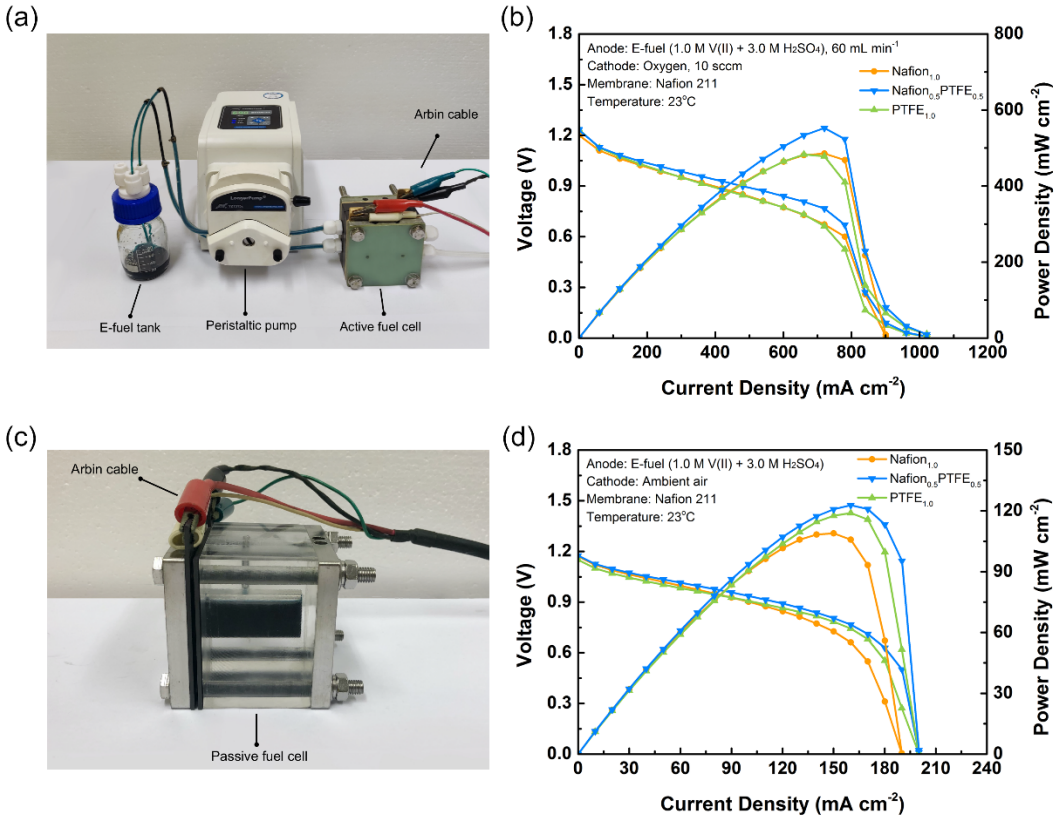

Fig. 5 Experimental set-up and polarization & power density curves of (a-b) the active and (c-d) the passive fuel cell assembled with three cathodes.

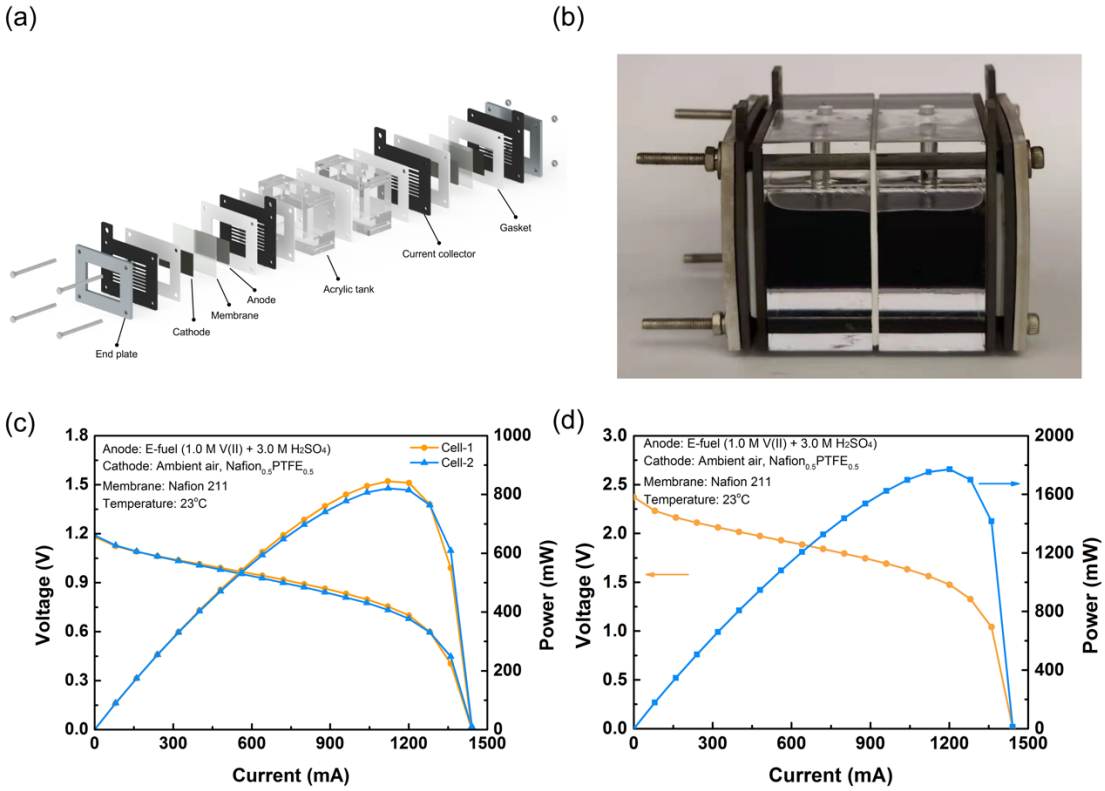

Fig. 6 (a) Design and (b) fabrication of a fuel cell stack. (c) The consistency of two individual cells. (d) General performance of this passive fuel cell stack.

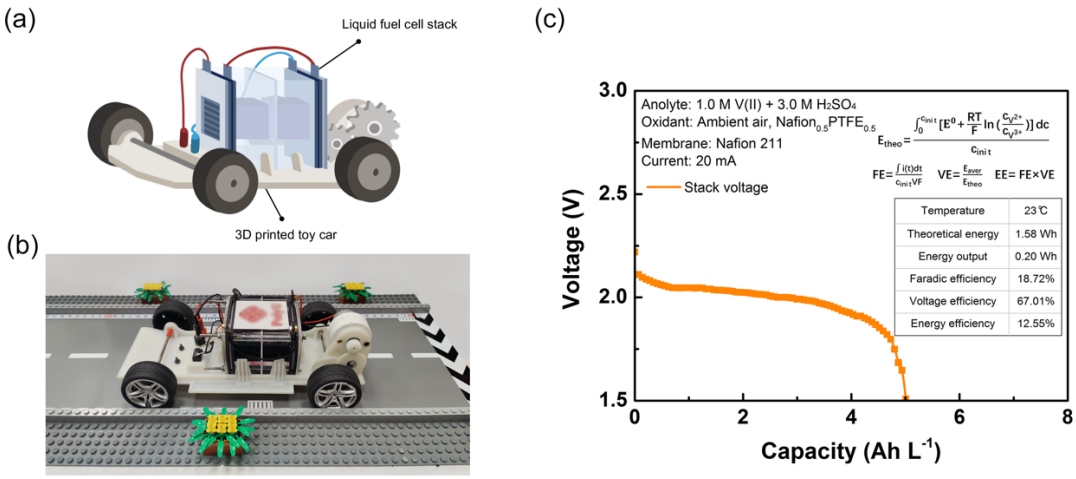

Fig. 7 (a) Design and (b) fabrication of a fuel cell powered toy car. (c) Constant-current discharging behaviors of the fuel cell stack.

Table of Contents Graphic: